

# PAH Formation under Single Collision Conditions: Reaction of Phenyl Radical and 1,3-Butadiene to Form 1,4-Dihydronaphthalene

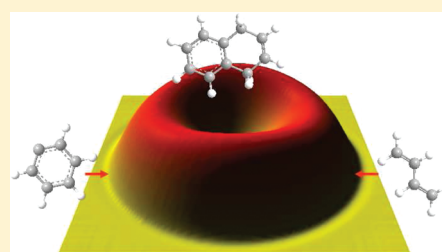
R. I. Kaiser,\* D. S. N. Parker, and F. Zhang

Department of Chemistry, University of Hawaii at Manoa, Honolulu, Hawaii 96822, United States

A. Landera, V. V. Kislov, and A. M. Mebel\*

Department of Chemistry & Biochemistry, Florida International University, Miami, Florida 33199, United States

**ABSTRACT:** The crossed beam reactions of the phenyl radical ( $C_6H_5$ ,  $X^2A_1$ ) with 1,3-butadiene ( $C_4H_6$ ,  $X^1A_g$ ) and D6-1,3-butadiene ( $C_4D_6$ ,  $X^1A_g$ ) as well as of the D5-phenyl radical ( $C_6D_5$ ,  $X^2A_1$ ) with 2,3-D2-1,3-butadiene and 1,1,4,4-D4-1,3-butadiene were carried out under single collision conditions at collision energies of about  $55 \text{ kJ mol}^{-1}$ . Experimentally, the bicyclic 1,4-dihydronaphthalene molecule was identified as a major product of this reaction ( $58 \pm 15\%$ ) with the 1-phenyl-1,3-butadiene contributing  $34 \pm 10\%$ . The reaction is initiated by a barrierless addition of the phenyl radical to the terminal carbon atom of the 1,3-butadiene to form a bound intermediate; the latter underwent hydrogen elimination from the terminal  $CH_2$  group of the 1,3-butadiene molecule leading to 1-phenyl-*trans*-1,3-butadiene through a submerged barrier. The dominant product, 1,4-dihydronaphthalene, is formed via an isomerization of the adduct by ring closure and emission of the hydrogen atom from the phenyl moiety at the bridging carbon atom through a tight exit transition state located about  $31 \text{ kJ mol}^{-1}$  above the separated products. The hydrogen atom was found to leave the decomposing complex almost parallel to the total angular momentum vector and perpendicularly to the rotation plane of the decomposing intermediate. The defacto barrierless formation of the 1,4-dihydronaphthalene molecule involving a single collision between a phenyl radical and 1,3-butadiene represents an important step in the formation of polycyclic aromatic hydrocarbons (PAHs) and their partially hydrogenated counterparts in combustion and interstellar chemistry.



## 1. INTRODUCTION

For the past few decades, the formation mechanisms of carbonaceous soot particles and their precursors such as polycyclic aromatic hydrocarbons (PAHs) have been the focus of extensive studies due to their importance in combustion, atmospheric, and interstellar chemistry.<sup>1–5</sup> Therefore it is of great interest to understand the underlying synthetic pathways to form PAHs and soot particles from the “bottom up” via atoms and radical precursors. It has been widely suggested that the phenyl radical in its ground electronic state ( $C_6H_5$ ,  $X^2A_1$ ) plays a crucial role in the formation of PAHs,<sup>6,7</sup> especially its reactions with unsaturated hydrocarbons such as (substituted) acetylenes, olefins, and aromatic molecules such as benzene.<sup>8–14</sup> Therefore, phenyl-type radical reactions have been included in chemical reaction networks modeling the formation of PAHs and related molecules in combustion processes<sup>1,15,16</sup> and in interstellar environments such as in circumstellar envelopes of carbon-rich stars (IRC+10216).<sup>4,17</sup> Depending on the temperature and pressure conditions, theoretical investigations coupled with kinetics studies of phenyl radical reactions indicate that the decomposition of the initial reaction intermediate, formed via addition of the phenyl radical to carbon–carbon double and/or triple bonds, can follow various routes: decomposition back to the reactants, fragmentation via atomic hydrogen loss pathways, isomerization, and/or stabiliza-

tion at higher pressures if the lifetime is long enough to allow third body collisions.<sup>18</sup> Recently, our group conducted systematic crossed molecular beam studies of the reaction of phenyl radicals with various unsaturated hydrocarbon molecules,<sup>19–22</sup> such as 1,3-butadiene,<sup>23</sup> utilizing a modified flash pyrolytic source<sup>24,25</sup> to produce phenyl radicals from a helium-seeded nitrosobenzene precursor. The flash pyrolysis approach generated phenyl radicals with high velocities from typically 2000 to 3000  $\text{ms}^{-1}$  and consequently high collision energies ( $117–149 \text{ kJ mol}^{-1}$  for the phenyl plus 1,3-butadiene reaction). Consequently, the reaction intermediates were relatively short-lived with lifetimes ranging from 0.1 to 4.5 ps; these lifetimes were found to be too short for successive isomerization and ring closure processes, and these reactions did not form any PAHs. Instead, the reaction of phenyl with 1,3-butadiene conducted at these high collision energies produced 1-phenyl-1,3-butadiene plus atomic hydrogen, but no bicyclic aromatic molecule.<sup>23</sup>

Besides crossed beam experiments at elevated collision energies, the reactions of phenyl radicals with various  $C_4H_6$  isomers have been investigated in flame experiments. In 2009,

**Received:** February 22, 2012

**Revised:** April 11, 2012

**Published:** April 12, 2012

Qi et al.<sup>26</sup> conducted a study of fuel-rich premixed toluene/argon/oxygen ( $C/O = 0.74$ ) flames at low temperatures of under 1000 K and pressures of 30 Torr, in which they identified several  $C_{10}H_{10}$  isomers including 2-butylnylbenzene, dialin, (*E*)-1-phenyl-1,3-butadiene, and 3-methylindene. Also, exploiting electronic structure calculations, Mebel et al.<sup>27</sup> studied the self-reaction of the cyclopentadienyl radical ( $c-C_5H_5$ ) to produce naphthalene through sequential atomic hydrogen loss reactions:  $c-C_5H_5 + c-C_5H_5 \rightarrow C_{10}H_{10} \rightarrow C_{10}H_9 + H/C_{10}H_8 + H_2$ . The authors suggested this route to be favored at temperatures below 1000 K; the alternative product fulvalene ( $C_{10}H_8$ ) could potentially contribute to the growth of cyclopentene-fused PAHs. In 2010, Kislov and Mebel<sup>28</sup> conducted an ab initio/RRKM-ME study on the mechanism and kinetics of the reaction of phenyl radicals with 1,2-butadiene. The results show that the reaction can either proceed via a direct hydrogen abstraction (preferable route) to produce benzene and (resonantly stabilized)  $C_4H_5$  radicals or through addition of the phenyl radical to distinct carbon atoms of  $H_2CCCHCH_3$  followed by isomerization of the  $C_{10}H_{11}$  collision complex and atomic hydrogen and methyl emission. The phenyl addition channels were calculated to be responsible for 10–30% of the total product yield, with their contribution decreasing as the temperature rises.

Recently, our group developed a photolysis source that generates a phenyl radical beam at velocities down to  $1600 \text{ ms}^{-1}$ ; this has enabled us to conduct crossed beam experiments with phenyl radicals such as with methylacetylene and allene at much lower collision energies of typically  $35\text{--}45 \text{ kJ mol}^{-1}$ .<sup>29–31</sup> These data presented compelling evidence that, in case of the phenyl–allene and phenyl–methylacetylene systems, a decrease of the collision energy dramatically changes the reaction dynamics and branching ratios of the products. Here, our experiments provided for the first time proof that an individual PAH—the indene molecule—can be formed as a result of a single collision event via indirect scattering dynamics in the gas phase. Whereas the phenyl–allene and phenyl–methylacetylene reactions depicted entrance barriers of about 1 and 14  $\text{kJ mol}^{-1}$ , respectively, the latest crossed beam study of the reaction of vinylacetylene ( $HCCC_2H_3$ ) with phenyl and D5-phenyl radicals conducted at a collision energy of 47 to 48  $\text{kJ mol}^{-1}$  showed that the PAH naphthalene ( $C_{10}H_8$ ) can be formed via a defacto barrierless reaction involving a van der Waals complex and submerged barrier to addition of the phenyl radical to the  $=CH_2$  group of vinylacetylene in the entrance channel.<sup>29</sup> These findings challenged conventional wisdom that PAH-formation only occurs at high temperatures such as in combustion systems or in outflows of carbon-rich stars and implies that a low temperature chemistry can initiate the synthesis of the very first PAH in cold molecular clouds at temperatures down to 10 K. These results and the presence of a  $=CH_2$  group in the C4 hydrocarbon 1,3-butadiene encouraged us to reinvestigate the reaction of phenyl radicals with 1,3-butadiene together with its partially deuterated reactants at much lower collision energies of 53 to 59  $\text{kJ mol}^{-1}$  to form the bicyclic 1,4-dihydro-naphthalene molecule together with its isomers under single collision conditions.

## 2. METHODS

**2.1. Experimental and Data Analysis.** The reactions of phenyl radicals  $C_6H_5(X^2A_1)$  with 1,3-butadiene ( $X^1A_g$ ) and D6-1,3-butadiene as well as D5-phenyl radicals with 2,3-D2-1,3-butadiene and 1,1,4,4-D4-1,3-butadiene were conducted in a

universal crossed molecular beams machine under single collision conditions at the University of Hawaii at Manoa.<sup>32–36</sup> Briefly, a supersonic beam of phenyl/D5-phenyl radicals seeded in helium (99.9999%; Gaspro) at fractions of about 1% was prepared by photodissociation of chlorobenzene/D5-chlorobenzene ( $C_6H_5Cl/C_6D_5Cl$ ; 99.9%; Fluka/Cambridge Isotopes) in the primary source chamber. This mixture was formed by passing 1.5 atm helium gas through chlorobenzene/D5-chlorobenzene stored in a stainless steel bubbler that was kept in a tempered water bath at 298 K. The gas mixture was then released by a Proch-Trickl pulsed valve operating with a 0.96 mm nozzle at 60 Hz, 80  $\mu\text{s}$  pulse width, and  $-400 \text{ V}$  to  $-450 \text{ V}$  pulse amplitude. The distance between the pulsed valve and skimmer was optimized to  $13 \pm 1 \text{ mm}$ . Chlorobenzene/D5-chlorobenzene molecules were then photodissociated by a 193 nm laser beam from a Lambda Physik Compex 110 Excimer laser operated at 60 Hz. The laser was operated with an output of  $10 \pm 1 \text{ mJ}$  per pulse focused by a 1 m quartz focus lens to  $4 \times 1 \text{ mm}$  before intercepting the molecular beam perpendicularly about 1 mm downstream of the nozzle. A four-slot chopper wheel was installed after the skimmer to select a part of the phenyl/D5-phenyl beam at a peak velocity ( $v_p$ ) of about  $1690 \text{ ms}^{-1}$  (Table 1). The radical

**Table 1. Primary and Secondary Beam Peak Velocities ( $v_p$ ), Speed Ratios ( $S$ ), Collision Energies ( $E_c$ ), and Center-of-Mass Angles ( $\Theta_{CM}$ )**

beam	$v_p$ ( $\text{ms}^{-1}$ )	$S$	$E_c$ $\text{kJ mol}^{-1}$	$\Theta_{MX}$
phenyl ( $X^2A_1$ )	$1690 \pm 20$	$8.6 \pm 0.5$		
1,3-butadiene ( $X^1A_g$ )	$770 \pm 20$	$8.0 \pm 0.5$	$55.3 \pm 1.1$	$17.6 \pm 0.5$
D5-phenyl ( $X^2A_1$ )	$1685 \pm 20$	$8.6 \pm 0.5$		
D6-1,3-butadiene ( $X^1A_g$ )	$750 \pm 20$	$8.0 \pm 0.5$	$58.6 \pm 1.2$	$19.0 \pm 0.5$
D4-1,3-butadiene ( $X^1A_g$ )	$750 \pm 20$	$8.0 \pm 0.5$	$53.6 \pm 1.2$	$18.5 \pm 0.5$
D2-1,3-butadiene ( $X^1A_g$ )	$750 \pm 20$	$8.0 \pm 0.5$	$53.6 \pm 1.2$	$17.9 \pm 0.5$

beam was perpendicularly intersected in the interaction region by the secondary pulsed molecular beam of 1,3-butadiene/D6-1,3-butadiene/2,3-D2-1,3-butadiene/1,1,4,4-D4-1,3-butadiene ( $C_4H_6$ , Sigma Aldrich, 99%; CDN, 99% D; 550 Torr) released by a second pulsed valve. In order to optimize the intensity of each supersonic beam, which strongly depends on the distance between the pulsed valve and the skimmer, on line and in situ, each pulsed valve was placed on a ultrahigh vacuum compatible micropositioning translation stage with three stepper motors (New Focus). This allowed for monitoring of the beam intensity versus the position of the pulsed valve in each source chamber on line and in situ. Since both beams are pulsed, the timing between the pulsed valves and photolysis laser had to be optimized. The pulsed valve in the primary source fired 1890  $\mu\text{s}$  after the chopper wheel sent its  $t = 0$  pulse; the laser was fired 162  $\mu\text{s}$  after the primary pulsed valve trigger, and the trigger to the secondary pulsed valve was initiated 1870  $\mu\text{s}$  after  $t = 0$ , i.e., 20  $\mu\text{s}$  prior to the primary pulsed valve.

The reactively scattered products were monitored using a triply differentially pumped quadrupole mass spectrometric detector in the time-of-flight (TOF) mode after electron-impact ionization of neutral species at 80 eV electron energy. The detector is rotatable in the plane defined by the primary and the secondary reactant beams to allow taking angular

resolved TOF spectra. At each angle, up to  $3 \times 10^6$  TOF spectra (up to 90 min per angle) were accumulated. The recorded TOF spectra were then integrated and normalized to extract the product angular distribution in the laboratory frame (LAB). In this setup, both the primary and secondary pulsed valves were operated at 120 Hz, but the photodissociation laser at only half the repetition rate of 60 Hz. This allowed for a background subtraction by taking TOF spectra in the “laser on” mode and subtracting from the TOF spectra recorded in the “laser off” mode. To extract information on the reaction dynamics, the experimental data must be transformed into the center-of-mass reference frame utilizing a forward-convolution routine.<sup>37,38</sup> This iterative method initially assumes an angular flux distribution,  $T(\theta)$ , and the translational energy flux distribution,  $P(E_T)$  in the center-of-mass system (CM). Laboratory TOF spectra and the laboratory angular distributions (LAB) were then calculated from the  $T(\theta)$  and  $P(E_T)$  functions and were averaged over a grid of Newton diagrams to account for the apparatus functions and the beam spreads in velocity and direction. Each diagram defines, for instance, the velocity and angular spread of each beam and the detector acceptance angle. Best fits were obtained by iteratively refining the adjustable parameters in the center-of-mass functions within the experimental error limits of, for instance, peak velocity, speed ratio, and error bars in the LAB distribution. The product flux contour map,  $I(\theta, u) = P(u) \times T(\theta)$ , reports the intensity of the reactively scattered products ( $I$ ) as a function of the CM scattering angle ( $\theta$ ) and product velocity ( $u$ ). This plot is called the reactive differential cross section and gives an image of the chemical reaction.

**2.2. Theoretical Calculations.** Geometries of all intermediates and transition states on the  $C_{10}H_{11}$  potential energy surface (PES) accessed via the reaction of phenyl radicals with 1,3-butadiene and the reactants and products were optimized using the hybrid density functional B3LYP method<sup>39,40</sup> with the 6-311G\*\* basis set. The same method was used to obtain vibrational frequencies, which were utilized to compute zero-point energy (ZPE) corrections, to characterize the stationary points as minima or first-order saddle points, and to calculate rate constants for unimolecular reaction steps. More accurate energies were computed using the G3(MP2,CC)//B3LYP version<sup>41,42</sup> of the original Gaussian 3 (G3) scheme<sup>43</sup> for high-level single-point energy calculations. The final energies at 0 K were obtained using the B3LYP optimized geometries and ZPE corrections according to the following formula:  $E_0[\text{G3}(\text{MP2,CC})] = E[\text{CCSD}(\text{T})/6\text{-}311\text{G}(\text{d,p})] + \Delta E_{\text{MP2}} + E(\text{ZPE})$ , where  $\Delta E_{\text{MP2}} = E[\text{MP2}/\text{G3large}] - E[\text{MP2}/6\text{-}311\text{G}(\text{d,p})]$  is the basis set correction and  $E(\text{ZPE})$  is the zero-point energy.  $\Delta E(\text{SO})$ , a spin-orbit correction, and  $\Delta E(\text{HLC})$ , a higher level correction, from the original G3 scheme were not included in our calculations, as they do not make significant contributions to relative energies. We used the Gaussian 98<sup>44</sup> program package for the B3LYP and MP2 calculations and the MOLPRO 2006<sup>45</sup> program package for the calculations of spin-restricted coupled cluster RCCSD(T) energies. For the entrance channel involving phenyl radical addition to the  $\text{CH}_2$  group of 1,3-butadiene, we additionally performed partial geometry optimization along the minimal energy reaction path (MEP) with the C–C distance for the forming bond fixed at different values between 2 and 4 Å and all other geometric parameters being optimized at the complete active space self-consistent-field (CASSCF) level<sup>46</sup> with the 6-311G\*\* basis set. The CASSCF active space consisted of nine electrons

distributed on nine orbitals, (9,9); typically, occupied orbitals with population numbers below 1.98 and vacant orbitals with population numbers above 0.02 were included. Vibrational frequencies for the partially optimized structures along the MEP were computed at the same CASSCF(9,9)/6-311G\*\* level. The CASSCF calculations were carried out using the DALTON 02 program package.<sup>47</sup> Then, dynamic correlation was taken into account via single-point multireference perturbation theory<sup>48</sup> (CASPT2/6-311G\*\*) calculations for each optimized structure along the path using MOLPRO 2006. A (7,7) active space was utilized in the CASPT2 calculations; all 26 occupied valence orbitals were included in single and double excitations.

Relative yields of various products of the reaction of phenyl radicals with 1,3-butadiene under single-collision conditions were evaluated employing Rice–Ramsperger–Kassel–Marcus (RRKM) calculations<sup>49–51</sup> of energy-dependent rate constants for individual unimolecular steps and of branching ratios of different products. The computational procedure was described in detail previously.<sup>52</sup> We calculated rate constants as functions of available internal energy of each intermediate or transition state; the internal energy was taken as the sum of the energy of chemical activation in the reaction of phenyl radicals with 1,3-butadiene and the collision energy, assuming that a dominant fraction of the latter is converted to internal vibrational energy. Only a single total-energy level was considered throughout, as for single-collision conditions (zero-pressure limit). The harmonic approximation was employed to compute numbers and densities of state needed for evaluating the rate constants. Using the calculated rate constants, we computed product branching ratios by solving first-order kinetic equations within the steady-state approximation for unimolecular isomerization and fragmentation steps of initial reaction intermediates formed as a result of the addition of phenyl to the carbon atoms C1 and C2 in 1,3-butadiene. From our experience, the uncertainties in calculated energies of up to  $10 \text{ kJ mol}^{-1}$  are typical for the G3 method employed here, which may result in uncertainties of the calculated branching ratios of about 10%.

### 3. RESULTS

**3.1. Laboratory Data.** In the crossed molecular beam reaction of phenyl radicals ( $C_6H_5$ ) with 1,3-butadiene,  $C_4H_6$ , the most intense reactive scattering signal was recorded at  $m/z = 130$ ; this corresponds to an ion of the empirical formula  $C_{10}H_{10}^+$  and can be attributed to a hydrogen atom loss pathway from a  $C_{10}H_{11}$  intermediate. Signal was also observed at  $m/z = 129$ , which corresponds to a molecular ion  $C_{10}H_9^+$ . Further inspection found that the lower intensity scattering signal at  $m/z = 129$  had superimposable TOF and LAB angular distributions profiles, after scaling, as the high intensity reactive scattering signal at  $m/z = 130$ . Superimposable TOF spectra were also observed for scattering signal measured at  $m/z = 116$  corresponding to  $C_9H_8^+$ , a potential methyl loss channel, and  $m/z = 104$  corresponding to  $C_8H_8^+$  as originating from a potential vinyl group loss channel. The signal at  $m/z = 116$  and  $m/z = 104$  had intensity of about 5% and 1%, respectively. Since the TOF spectra are identical within the detection and signal-to-noise limits of our system, we can state that the signal at lower  $m/z$  values (129, 116, and 104) originate from dissociative ionization of the major reaction product  $C_{10}H_{10}$  in the electron impact ionizer. The TOFs for the reaction of phenyl radicals ( $C_6H_5$ ) with 1,3-butadiene ( $C_4H_6$ ) forming  $C_{10}H_{10}$  isomers at  $m/z = 130$  are shown in Figure 1 with the

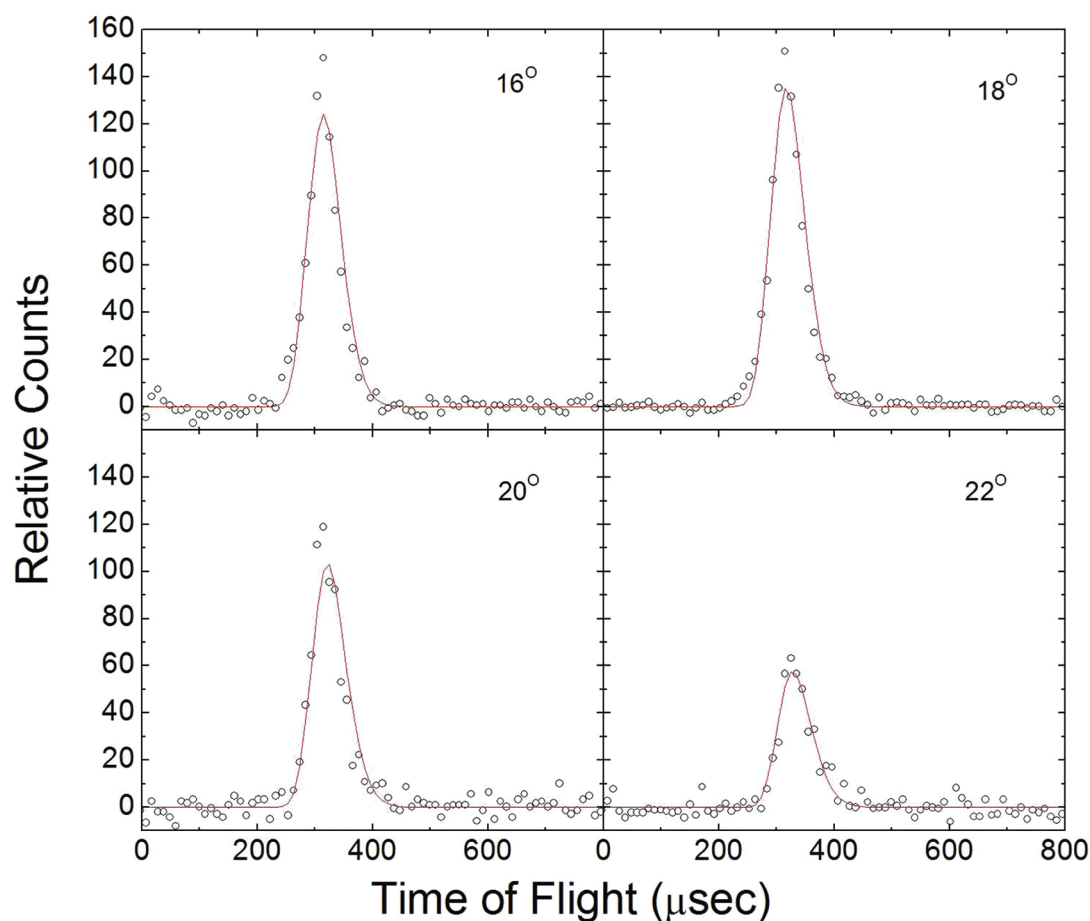


**Figure 1.** TOF data recorded at  $m/z = 130$  ( $C_{10}H_{10}^+$ ) for the reaction of phenyl radicals ( $C_6H_5$ ;  $X^2A_1$ ) with 1,3-butadiene ( $C_4H_6$ ;  $X^1A_2$ ) at various laboratory angles at a collision energy of  $55.3 \text{ kJmol}^{-1}$ . The circles represent the experimental data, and the solid line represents the fit.

LAB angular distribution depicted in Figure 2. The laboratory data in Figures 1 and 2 were fit with a single channel with a mass combination of 130 amu ( $C_{10}H_{10}$ ) and 1 amu (H) to give the center-of-mass angular and translational distributions depicted in Figure 3. Therefore, based on the mass combination

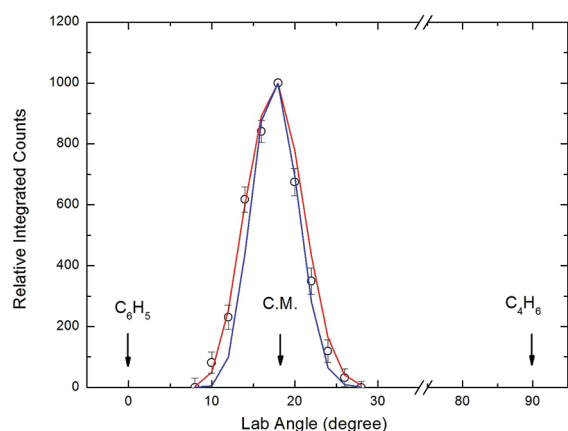


**Figure 2.** Laboratory angular distribution recorded at  $m/z = 130$  ( $C_{10}H_{10}^+$ ) for the reaction of phenyl radicals ( $C_6H_5$ ;  $X^2A_1$ ) with 1,3-butadiene ( $C_4H_6$ ;  $X^1A_2$ ). Solid circles represent the experimental data together with  $1\sigma$  error bars. The solid red line corresponds to the calculated best fit distribution for the 1,4-dihydronaphthalene product isomer; the solid blue line presents the simulation assuming that the 1-phenyl-1,3-butadiene isomer is formed.

of the products alone, we can state that within the detection limit of our machine, only a hydrogen emission pathway is open.

We have elucidated that the major reactive scattering signal originates from atomic hydrogen emission, but does this hydrogen loss come from the phenyl radical or from the 1,3-butadiene molecule, and if it is emitted from the latter, is it from the terminal (C1/C4) and/or center (C2/C3) positions? In a process of elimination, we used deuterated and partially deuterated reactants to ascertain the location(s) of the position of the hydrogen emission. First, the reactive scattering signal from the reaction of phenyl ( $C_6H_5$ ) with D6-1,3-butadiene at  $m/z = 136$  ( $C_{10}D_6H_4^+$ ) was measured; this signal corresponds to a hydrogen atom emission from the phenyl ring. The TOF spectra and LAB distribution are shown in Figures 4 and 5, respectively. These data could be fit with identical center-of-mass functions as those for the phenyl plus 1,3-butadiene system shown in Figure 3. The intensity of the hydrogen loss from the partially deuterated reaction was found to be  $58 \pm 15\%$  of that of the fully hydrogenated system as seen by comparisons of Figures 1 and 4. This suggests that the hydrogen atom is at least emitted from the phenyl ring and, based on the intensities, also from 1,3-butadiene. However, the absolute intensity of the hydrogen loss channel suggests that at least one other pathway must be involved.

To further investigate to what extent hydrogen emission occurred from the 1,3-butadiene molecule, the hydrogen loss channel was monitored in the reaction of partially deuterated

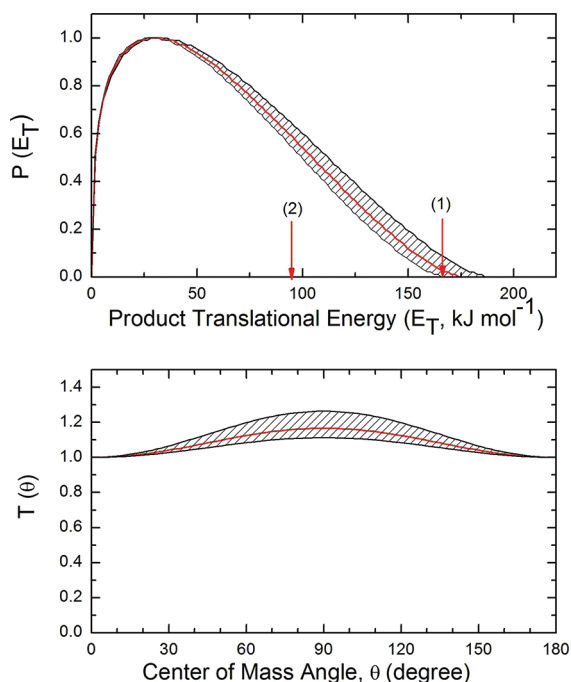


**Figure 3.** Center-of-mass angular (bottom) and translational energy flux distributions (top) of the reaction of phenyl radicals ( $C_6H_5$ ;  $X^2A_1$ ) with 1,3-butadiene ( $C_4H_6$ ;  $X^1A_g$ ) utilized to fit the laboratory data as shown in Figures 1 and 2. Hatched areas indicate the acceptable upper and lower error limits of the fits. The red line defines the best fit functions. (1) and (2) indicate the predicted high energy cutoffs for the formation of the 1,4-dihydronaphthalene and 1-phenyl-1,3-butadiene isomers, respectively.

1,3-butadiene molecules with D5-phenyl radicals. These reactions were conducted to locate whether emission occurred from the  $CH_2$  end group (C1/C4) or from the CH group (C2/C3) in the center of 1,3-butadiene. Here, the hydrogen emission from the  $CH_2$  group was monitored by measuring the absolute reactive scattering signal at the center-of-mass angle, at  $m/z = 137$  ( $C_{10}H_3D_7^+$ ), in the reaction of 2,3-D2-1,3-butadiene with D5-phenyl (Figure 6). To monitor the hydrogen loss from the central carbon atoms, the reactive scattering signal was measured at  $m/z = 139$  ( $C_{10}HD_9^+$ ) in the reaction of 1,1,4,4-D4-1,3-butadiene with D5-phenyl (Figure 6). Here, reactive scattering signal was seen in both reactions; the intensity of the hydrogen atom emission from the  $CH_2$  group ( $m/z = 137$   $C_{10}H_3D_7^+$ ) was about  $43 \pm 10\%$  of the signal of the hydrogen loss of the phenyl-1,3-butadiene system; the hydrogen atom emission from the CH group ( $m/z = 139$ ) was only  $10 \pm 5\%$  of the signal of the hydrogen loss of the phenyl-1,3-butadiene system. What conclusions can we draw from these numbers? First of all, the intensity of the signal  $m/z = 139$  is, within the error limits, explainable with a deuterium atom elimination from the  $^{13}CC_9H_2D_9$  intermediate forming  $^{13}CC_9H_2D_8$ ; recall that  $^{13}C$  occurs with natural abundances of 1.1%, and for a molecule with 10 carbon atoms, the fraction of one molecule carrying one  $^{13}C$  is 11%. Therefore, we have no compelling evidence of a hydrogen atom elimination from the C2/C3 carbon atoms of the 1,3-butadiene molecule, since the signal at the level of  $10 \pm 5\%$  might be explained by the  $^{13}C$  substituted  $^{13}CC_9H_2D_8$  product. Second, the reactive scattering signal at  $m/z = 137$  ( $43 \pm 10\%$  of the signal of the hydrogen loss of the phenyl-1,3-butadiene system) could partly originate by about 11% from the formation of  $^{13}CC_9H_4D_6^+$ , thus reducing the

relative intensity of the hydrogen loss from the C1/C4 carbon atoms to about  $32 \pm 10\%$  compared to the fully hydrogenated system. With about  $32 \pm 10\%$  of the hydrogen coming from the C1/C4 position (result from the phenyl -2,3-D2-1,3-butadiene) and about  $58 \pm 15\%$  from the phenyl group (result from the phenyl - D6-1,3-butadiene), this accounts for about  $90 \pm 25\%$  of the hydrogen detected via the partially deuterated reactants compared to the fully hydrogenated system, thus accounting, within the error limits, for the hydrogen balance.

**3.2. Center-of-Mass Frame.** Having identified the molecular masses of the reaction product(s) ( $m/z = 130$ ) and hence its empirical formulas to be  $C_{10}H_{10}$  for the reaction of the phenyl radical with 1,3-butadiene and that the hydrogen elimination originates predominantly from the phenyl radical ( $58 \pm 15\%$ ) and to a lesser extent from the C1/C4 position of the 1,3-butadiene molecule ( $32 \pm 10\%$ ), we are attempting now to extract information on the underlying reaction dynamics. This is achieved by converting the laboratory data into the center-of-mass reference frame and analyzing the resulting center-of-mass angular  $T(\theta)$  and translational energy  $P(E_T)$  distributions. The simulated distributions (TOF, laboratory angular distribution) are overlaid on the experimental data in Figures 1 and 2 and Figures 4 and 5 with the corresponding center-of-mass functions visualized in Figure 3. For the  $C_6H_5$  plus 1,3- $C_4H_6$  system, the recorded TOF spectra and laboratory angular distribution were fit with a single channel of the product mass combination 130 amu ( $C_{10}H_{10}$ ) plus 1 (H) amu by utilizing parametrized center-of-mass angular distributions and center-of-mass translational energy distributions. The center of mass angular distribution,  $T(\theta)$ , depicts intensity over the complete angular range from  $0^\circ$  to  $180^\circ$ ; further, within the error limits, all fits are symmetric and with a maximum at  $90^\circ$ . These findings indicate that the reaction involves indirect scattering dynamics via the formation of bound  $C_{10}H_{11}$  reaction intermediate(s).<sup>53</sup> Also, the symmetry of the  $T(\theta)$  suggests that the lifetime of the intermediate(s) is longer than its (their) rotational period.<sup>54</sup> Further, the maximum at  $90^\circ$  indicates geometrical constraints when the reaction intermediate decomposes, i.e., a preferential hydrogen loss parallel to the total angular momentum vector and almost perpendicularly to the rotational plane of the decomposing intermediate.<sup>53</sup>

The center-of-mass translational energy distribution,  $P(E_T)$ , provides us with additional information on the reaction dynamics. For this system, the  $P(E_T)$  extends up to a maximum translational energy of  $175 \text{ kJ mol}^{-1}$  (Figure 3). Adding or subtracting  $30 \text{ kJ mol}^{-1}$  does not change the fit significantly. Since the high energy cutoff represents the sum of the reaction energy and the collision energy, we can subtract the collision energy of  $55 \text{ kJ mol}^{-1}$  to compute the reaction energy to be exoergic by  $120 \pm 30 \text{ kJ mol}^{-1}$ . Second, the  $P(E_T)$  holds a broad maximum of about  $30 - 40 \text{ kJ mol}^{-1}$ . This finding suggests the existence of at least one reaction channel holding a tight exit barrier upon decomposition of the  $C_{10}H_{11}$  intermediate(s). Finally, by integrating the center-of-mass translational energy distribution and accounting for the available energy, the average fraction of available energy channeling into the translational degrees of freedom is computed to be  $35 \pm 4\%$ . This order of magnitude indicates indirect scattering dynamics via complex formation in agreement with the laboratory and center-of-mass angular distributions. The fit to the experimental data was found to be insensitive to the entrance barrier parameter, which could be

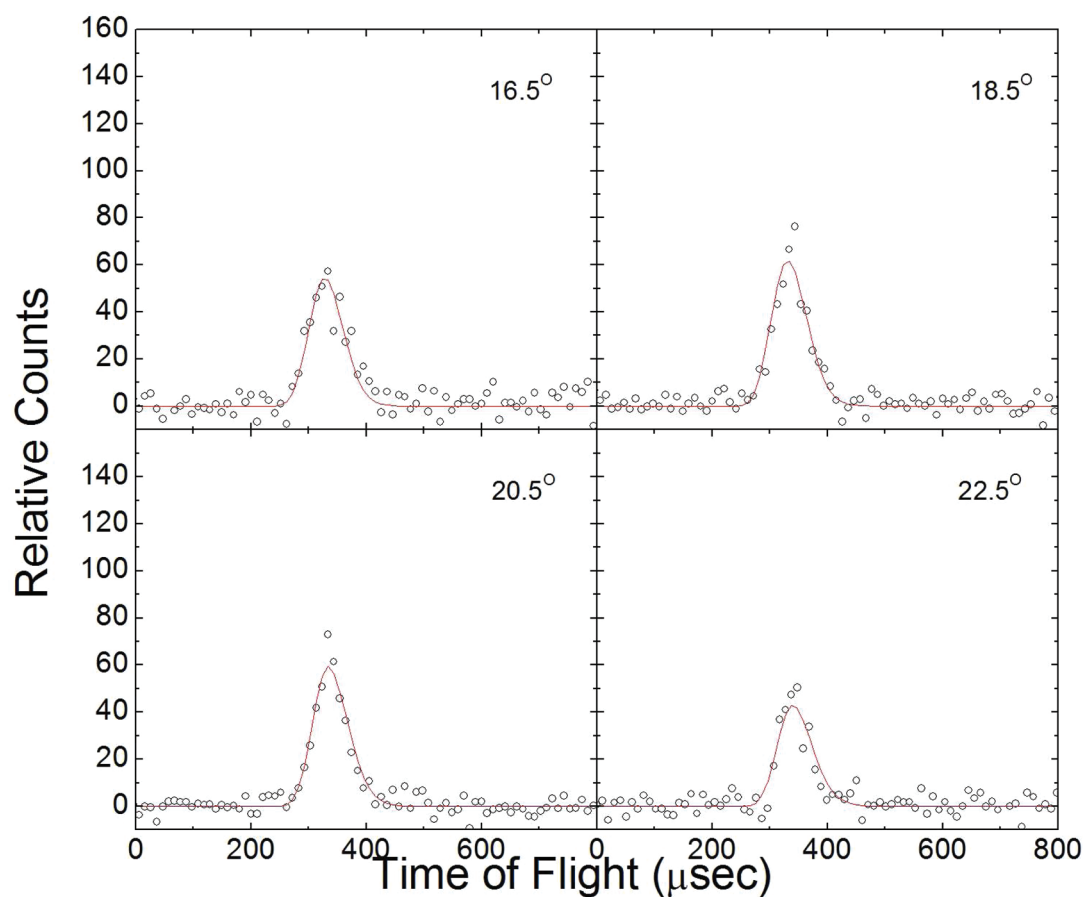


**Figure 4.** TOF data recorded at  $m/z = 136$  ( $C_{10}H_4D_6^+$ ) for the reaction of phenyl radicals ( $C_6H_5$ ;  $X^2A_1$ ) with D6-1,3-butadiene ( $C_4D_6$ ;  $X^1A_g$ ) at various laboratory angles at a collision energy of  $58.6 \text{ kJ mol}^{-1}$ . The circles represent the experimental data and the solid line the fit.

fit with either no entrance barrier or with a small entrance barrier of up to  $15 \text{ kJ mol}^{-1}$ . As a combined result of the two center of mass functions, the flux contour maps of this reaction derived from the best fit functions are also shown in Figure 7.

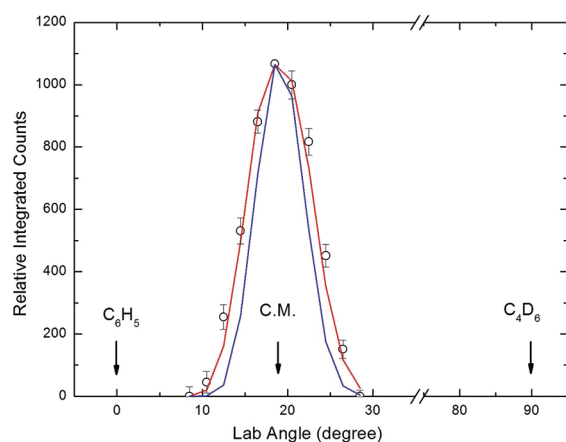


**Figure 5.** Laboratory angular distribution recorded at  $m/z = 136$  ( $C_{10}H_4D_6^+$ ) for the reaction of phenyl radicals ( $C_6H_5$ ;  $X^2A_1$ ) with D6-1,3-butadiene ( $C_4D_6$ ;  $X^1A_g$ ). Solid circles represent the experimental data together with  $1\sigma$  error bars. The solid red line corresponds to the calculated best fit distribution for the partially deuterated 1,4-dihydronaphthalene product isomer; the solid blue line presents the simulation assuming that the partially deuterated 1-phenyl-1,3-butadiene isomer is formed.

For the  $C_6H_5$  plus 1,3- $C_4D_6$  system, the experimental data at  $m/z = 136$  could be fit with one channel with the mass combination of 136 ( $C_{10}D_6H_4$ ) and 1 (H) amu. The center-of-mass functions are identical to those used in the  $C_6H_5$  plus 1,3- $C_4H_6$  system.

## 4. DISCUSSION

**4.1. Product Isomer Identification.** From the laboratory data alone, we can identify the formation of  $C_{10}H_{10}$  isomer(s) plus atomic hydrogen. By considering the energetics of the reaction and, consequently, the energy of product formation, we can identify the product isomer by comparing the experimentally determined reaction energy of  $120 \pm 30 \text{ kJ mol}^{-1}$  with theoretically calculated energies for distinct  $C_{10}H_{10}$  isomers. Here, the experimentally determined reaction exoergicity of  $120 \pm 30 \text{ kJ mol}^{-1}$  matches the theoretically predicted one for the 1,4-dihydronaphthalene isomer of  $98 \pm 10 \text{ kJ mol}^{-1}$  within the error limits (Figure 8). The second closest exoergic product isomer is the monocyclic 1-phenyl-*trans*-1,3-butadiene and an associated reaction energy of  $-36 \text{ kJ mol}^{-1}$ , some  $84 \text{ kJ mol}^{-1}$  higher in energy than that observed in the experiments. Therefore, based on the energetics alone, we can conclude that at least the thermodynamically more stable 1,4-dihydronaphthalene isomer is formed. To further verify the dominant formation of this isomer, we created a parameter file for conversion of the laboratory data to center-of-mass frame data with a product formation energy of  $-36 \text{ kJ mol}^{-1}$  corresponding to the monocyclic 1-phenyl-*trans*-1,3-butadiene

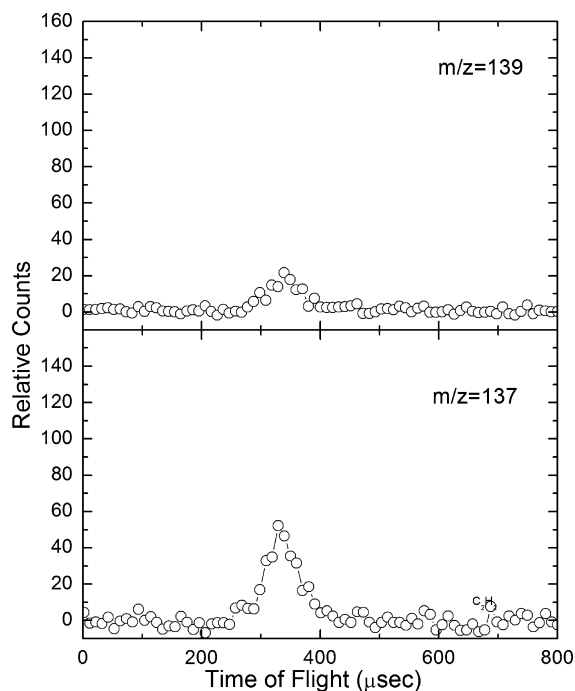


**Figure 6.** Bottom: TOF spectrum recorded at the center-of-mass angle at  $m/z = 137$  ( $C_{10}H_3D_7^+$ ) during the reaction of D5-phenyl ( $C_6D_5$ ;  $X^2A_1$ ) with 2,3-D2-1,3-butadiene. Top: TOF spectrum recorded at the center-of-mass angle at  $m/z = 139$  ( $C_{10}HD_9^+$ ) in the crossed beam reaction of D5-phenyl ( $C_6D_5$ ;  $X^2A_1$ ) with 1,1,4,4-D4-1,3-butadiene.

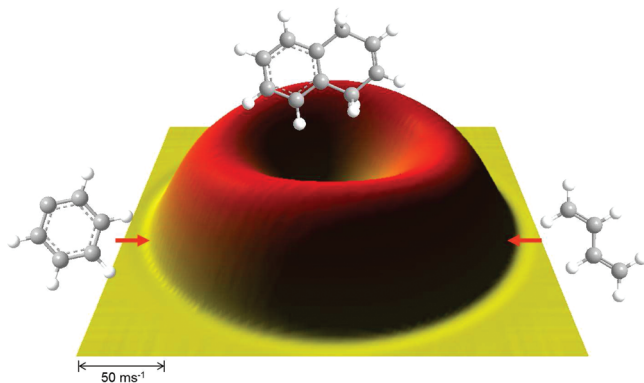


**Figure 7.** Flux contour map of the reaction of phenyl radicals ( $C_6H_5$ ;  $X^2A_1$ ) with 1,3-butadiene ( $C_4H_6$ ;  $X^1A_g$ ) utilized to fit the laboratory data as shown in Figures 1 and 2.

to see the effect on the lab angular distribution. The fit is represented by the blue line in Figures 2 and 5; this shows a much narrower laboratory distribution, which hardly reproduces the experimental data. This provides evidence that 1-phenyl-*trans*-1,3-butadiene is not the predominant experimental product, but it could form a minor proportion of the signal.

**4.2. Proposed Reaction Dynamics.** Before we untangle the reaction dynamics, we would like to summarize the results obtained.

**R1:** In the phenyl-1,3-butadiene system, the experimental data suggest the formation of a  $C_{10}H_{10}$  isomer via hydrogen atom elimination involving indirect scattering dynamics through a long-lived  $C_{10}H_{11}$  intermediate and a tight exit transition state; the hydrogen atom loss occurred parallel to the total angular momentum vector and almost perpendicularly to the rotation plane of the decomposing complex. A comparison

of the experimentally determined reaction energy with the theoretically obtained one suggests at least the formation of the thermodynamically more stable 1,4-dihydronaphthalene isomer with potential lower contributions from the 1-phenyl-*trans*-1,3-butadiene isomer.

**R2:** In the phenyl-D6-1,3-butadiene system, the experimental data suggest an atomic hydrogen loss from the phenyl group. The intensity of this channel is  $58 \pm 15\%$  of the intensity for the phenyl-1,3-butadiene system. This together with the fact that both the phenyl-1,3-butadiene and phenyl-D6-1,3-butadiene systems could be fit with identical center-of-mass functions indicate that the 1,4-dihydronaphthalene isomer is most likely the dominant reaction product formed and that the hydrogen atom is emitted predominantly from the phenyl moiety.

**R3:** In the D5-phenyl-1,1,4,4-D4-1,3-butadiene system, the intensity of the signal at  $m/z = 139$  could be predominantly explained within the error limits by a deuterium elimination channel and formation of  $^{13}CC_9H_2D_8^+$ . Therefore, in this system, within our limits, no compelling evidence for a hydrogen elimination from the C2/C3 carbon atoms of the 1,1,4,4-D4-1,3-butadiene reactant and inherent formation of  $C_{10}HD_9$  could be provided.

**R4:** In the D5-phenyl-2,3-D2-1,3-butadiene system, the intensity of the signal at  $m/z = 137$  could be predominantly explained by a hydrogen atom emission and formation of  $C_{10}H_3D_7$ , i.e., a hydrogen emission from the  $CH_2$  group of the C1 and C4 atoms of 2,3-D2-1,3-butadiene. A comparison of the absolute intensities of the hydrogen loss from the phenyl group (1,4-dihydronaphthalene) indicates a fraction of the hydrogen loss from the terminal  $CH_2$  groups of about  $32 \pm 10\%$ ; this leads to the formation of the 1-phenyl-1,3-butadiene isomer.

We now turn our attention to the reaction mechanism suggested by the calculated PES as shown in Figure 8. According to the calculations, the phenyl radical addition to the C1 carbon of 1,3-butadiene occurs without a barrier to produce intermediate **i1**, residing  $193 \text{ kJ mol}^{-1}$  below the initial reactants. The addition transition state was located at the B3LYP/6-311G\*\* level of theory, which gives the corresponding barrier as  $3.7 \text{ kJ mol}^{-1}$  with ZPE corrections included. However, at the G3(CC,MP2) level, the transition state energy is  $2.0 \text{ kJ mol}^{-1}$  lower than the energy of the reactants, likely indicating a barrierless character of the reaction. The absence of the entrance barrier is supported by the results of multi-reference CASPT2(7,7)//CASSCF(9,9)/6-311G\*\* calculations of the MEP, which showed an attractive character of the potential when the phenyl radical approaches the terminal (C1) carbon, until a van der Waals complex stabilized by  $25 \text{ kJ mol}^{-1}$  with respect to the reactants is formed at the C–C distance of  $\sim 3.0 \text{ \AA}$ . As the carbon–carbon distance continues to decrease, the system goes via a submerged barrier located  $3 \text{ kJ mol}^{-1}$  above the complex, but  $22 \text{ kJ mol}^{-1}$  below the reactants. The intermediate **i1** can lose a hydrogen atom from the attacked C1 carbon to form 1-phenyl-*trans*-1,3-butadiene (**p1**) with the overall exothermicity of  $36 \text{ kJ mol}^{-1}$  and the hydrogen atom loss transition state residing  $21 \text{ kJ mol}^{-1}$  below the reactants but  $15$  and  $172 \text{ kJ mol}^{-1}$  above **p1** + H and **i1**, respectively. Alternatively, **i1** can undergo rotation around the CH–CH bond in the side-chain to form a nearly isoenergetic isomer **i2** via a relatively low barrier of  $57 \text{ kJ mol}^{-1}$ . **i2** can also lose a hydrogen atom from the same  $CH_2$  group as in **i1** producing 1-phenyl-*cis*-1,3-butadiene (**p2**) + H lying  $23 \text{ kJ mol}^{-1}$  lower in energy than phenyl plus 1,3-butadiene, via a

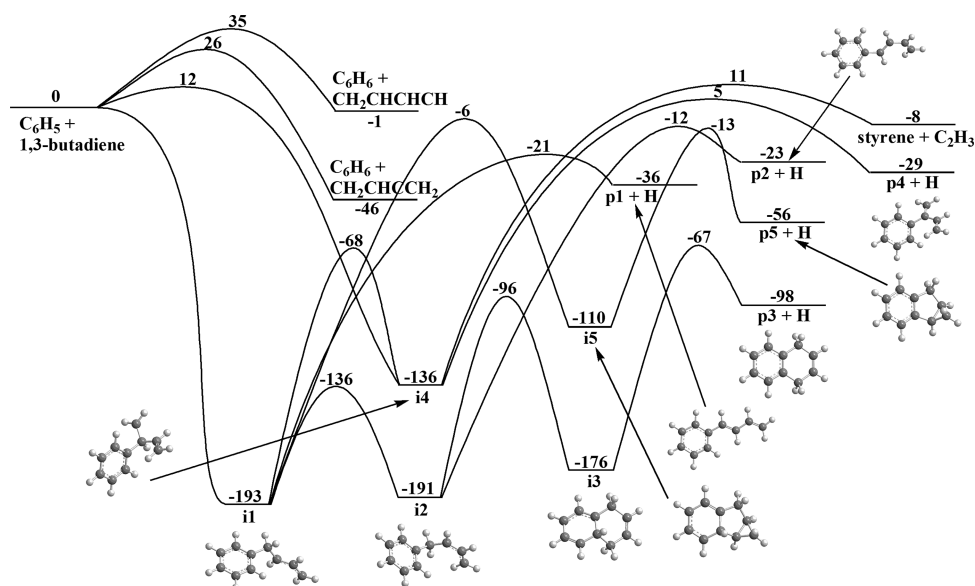


**Figure 8.**  $C_{10}H_{11}$  PES relevant to the reaction of phenyl radicals with 1,3-butadiene computed at the G3(MP2,CC)//B3LYP/6-311G\*\* level of theory. Relative energies are given in  $\text{kJ mol}^{-1}$ .

transition state located  $12 \text{ kJ mol}^{-1}$  below the reactants. However, a more favorable isomerization route from **i2** is its ring closure to **i3** ( $176 \text{ kJ mol}^{-1}$  below the reactants, via a barrier of only  $95 \text{ kJ mol}^{-1}$ ,  $84 \text{ kJ mol}^{-1}$  lower than that for the H loss. In turn, **i3** can decompose to the most thermodynamically favorable product 1,4-dihydronaphthalene (**p3**) by atomic hydrogen loss from the initial phenyl ring. Here, **p3** plus the hydrogen and the hydrogen atom elimination transition state reside  $98$  and  $67 \text{ kJ mol}^{-1}$  below the reactants. The phenyl plus 1,3-butadiene reaction can also start with phenyl radical addition to the C2 carbon. In this case, the reaction barrier is computed to be  $12 \text{ kJ mol}^{-1}$ , and the intermediate **i4** produced lies  $136 \text{ kJ mol}^{-1}$  lower in energy than the reactants. It is noteworthy that **i1** and **i4** can rearrange to one another by migration of the phenyl moiety over the  $\text{C}=\text{C}$  bond via a transition state at  $-68 \text{ kJ mol}^{-1}$  relative to the reactants. **i4** can also lose the hydrogen atom from the attacked CH group forming 2-phenyl-1,3-butadiene (**p4**) (exothermic by  $29 \text{ kJ mol}^{-1}$ ) or eliminate the vinyl radical ( $\text{C}_2\text{H}_3$ ) producing styrene (exothermic by  $8 \text{ kJ mol}^{-1}$ ). However, the atomic hydrogen and vinyl loss barriers from **i4** are high,  $141$  and  $147 \text{ kJ mol}^{-1}$ , i.e., respectively  $73$  and  $79 \text{ kJ mol}^{-1}$  higher than the barrier for the **i4**  $\rightarrow$  **i1** rearrangement. Finally, a direct hydrogen atom abstraction by the phenyl radical from 1,3-butadiene can produce benzene together with  $\text{CH}_2\text{CHCCH}_2$  and  $\text{CH}_2\text{CHCHCH}$ , exothermic by  $46$  and  $1 \text{ kJ mol}^{-1}$  via barriers of  $26$  and  $35 \text{ kJ mol}^{-1}$ , respectively.

We would like to note that previous computations suggested that intermediate **i1** can isomerize to a tricyclic structure **i5**, which was proposed to further isomerize to a 1-hydro-1-methylindene radical by 1,3-H shift from the bridging CH group common for the five- and six-member rings to  $\text{CH}_2$  in the three-member ring. 1-hydro-1-methylindene then eventually decomposes to indene by methyl group loss or, via hydrogen atom emission, to form 1-methylindene.<sup>55</sup> We were able to reproduce the transition state suggested by Fascella et al.<sup>55</sup> to connect **i5** with 1-hydro-1-methylindene; however, our intrinsic reaction coordinate (IRC) calculations showed that this transition state represents a hydrogen loss transition state

linking **i5** with a tricyclic product **p5**. No transition state for the 1,3-H shift in **i5** could be found despite a careful search. We conclude that 1-hydro-1-methylindene can be formed only via a secondary reaction of hydrogen addition to the  $\text{CH}_2$  group in the three-member ring of **p5** occurring via a high barrier of  $76 \text{ kJ mol}^{-1}$ . Thus, the 1-hydro-1-methylindene intermediate cannot be reached in the primary phenyl plus 1,3-butadiene reaction, and therefore a path to the formation of indene does not exist here. Moreover, the barrier for the **i1**  $\rightarrow$  **i5** isomerization is  $15 \text{ kJ mol}^{-1}$  higher than that for the hydrogen atom loss from **i1** to form **p1**, and rate constant calculations for the ring closure of **i1** to **i5** suggest that this pathway cannot compete with the other isomerization/dissociation channels of **i1**.

It should be noted that the G3(MP2,CC) energetics calculated here significantly differs from the B3LYP/6-31G\*\* results reported earlier by Ismail et al.,<sup>14</sup> whereas the agreement with the G2MP2 results by Fascella et al.<sup>55</sup> is reasonable, within  $5$ – $19 \text{ kJ mol}^{-1}$ . For example, the exoergicity of the 1,4-dihydronaphthalene (**p3**) plus atomic hydrogen is computed to be  $98$ ,  $109$ , and  $70 \text{ kJ mol}^{-1}$  at the G3(MP2,CC), G2MP2, and B3LYP/6-31G\*\* levels, respectively, the first two values being much closer to the experimental reaction exothermicity of  $120 \pm 30 \text{ kJ mol}^{-1}$  from the present crossed molecular beams experiment. Also, the difference in relative energies of the atomic hydrogen loss transition states from **i1** and **i3** is  $46$  and  $42 \text{ kJ mol}^{-1}$  at G3(MP2,CC) and G2MP2, respectively, versus  $23 \text{ kJ mol}^{-1}$  at B3LYP; such a discrepancy may significantly affect statistical product branching ratios computed from RRKM rate constants. While the G3(MP2,CC) method is generally known to be more reliable than B3LYP for relative energies, we can confirm the accuracy of our calculations by comparing with available experimental thermochemical data. For instance, using NIST enthalpies of formation for phenyl ( $339 \pm 8 \text{ kJ mol}^{-1}$ ), 1,3-butadiene ( $108.8 \pm 0.8 \text{ kJ mol}^{-1}$ ), styrene ( $146.9 \pm 1.0 \text{ kJ mol}^{-1}$ ), and vinyl ( $299 \pm 5 \text{ kJ mol}^{-1}$ ),<sup>56</sup> the experimental exothermicity for the styrene plus vinyl channel is  $2 \text{ kJ mol}^{-1}$ , close to the G3(MP2,CC) calculated value of  $8 \text{ kJ mol}^{-1}$ . The best available experimental<sup>57</sup> and

theoretical<sup>58</sup> enthalpies of formation of 1,4-dihydronaphthalene are close, 138.8 and 138.4 kJ mol<sup>-1</sup>, respectively, and using these values together with the NIST data, the **p3** plus atomic hydrogen products are exothermic by ~91 kJ mol<sup>-1</sup>, that is, within 7 kJ mol<sup>-1</sup> from our G3(MP2,CC) result. On the basis of this comparison and the usual accuracy expected from G3(MP2,CC),<sup>41–43</sup> we can conclude that the relative energies presented here should be accurate at least within ±10 kJ mol<sup>-1</sup>.

Further, the product branching ratios computed at various collision energies are shown in Table 2. One can see that 1,4-

**Table 2. Statistical Branching Ratios (%) of Various Products in the Phenyl Plus 1,3-Butadiene Reaction Computed at Different Collision Energies**

products	collision energy, kJ mol <sup>-1</sup>				
	0	30	55	117	149
<b>p1</b> + H	0.06	1.31	5.68	32.44	45.56
<b>p2</b> + H	0.00	0.12	0.80	8.26	13.70
<b>p3</b> + H	99.94	98.57	93.51	58.92	39.77
<b>p4</b> + H	0.00	0.00	0.00	0.08	0.18
<b>p5</b> + H	0.00	0.00	0.00	0.00	0.00
styrene + vinyl	0.00	0.00	0.01	0.31	0.79

dihydronaphthalene (**p3**) clearly dominates at low collision energies. At the present conditions of the crossed molecular beams experiment ( $E_{\text{col}} = 55 \text{ kJ mol}^{-1}$ ), the calculated statistical branching ratios qualitatively agree with experiment, but the relative yield of **p3**, 93.5%, is overestimated, whereas those of 1-phenyl-1,3-butadienes (**p1** and **p2**), 5.7% and 0.8%, respectively, are underestimated. This quantitative disagreement may be partially due to a deviation from the statistical behavior, as the dynamical factors clearly favor the immediate hydrogen atom loss from **i1** to form **p1** and thus would increase the branching ratio of the latter. The kinetic isotope effect on the branching ratios is relatively small. Since the C–H bond is slightly weaker than the C–D bond due to the difference in zero point energies, in the reactions involving deuterated molecules, the relative energies of the products obtained by a deuterium atom elimination and the corresponding deuterium loss transition states increase by 6–8 kJ mol<sup>-1</sup> as compared to those computed for the nondeuterated phenyl plus 1,3-butadiene system and shown in Figure 8, whereas changes in the relative energies for all other species on the PES do not exceed 1 kJ mol<sup>-1</sup>. As a result, the relative yields of the products obtained by the deuterium loss decrease by 1–3% and those from the hydrogen atom loss accordingly increase. At high collision energies, as in the previous crossed beams experiments,<sup>23</sup> the 1-phenyl-1,3-butadiene products eventually become dominant, even if the system continues to behave statistically. It should also be noted that the product branching ratios appeared to be practically independent of the initial decomposing intermediate (**i1** or **i4** for the phenyl radical addition to C1 or C2 carbons in 1,3-butadiene, respectively), because **i4** rearranges to **i1** much faster than it dissociates.

We combine now the experimental results with the computations and propose the underlying chemical dynamics of the reaction of the phenyl radical with 1,3-butadiene. The reaction follows indirect scattering dynamics and is initiated by an addition of the phenyl radical to the C1 and C2 carbon atoms of the 1,3-butadiene molecule forming intermediates **i1** and **i4**, respectively. At the low-temperature conditions of interstellar clouds of 10 K, only the barrierless addition to C1

forming **i1** is open, whereas elevated temperatures and the conditions (collision energy) of our crossed beam experiments also open up the addition to C2, yielding **i4**. Nevertheless, our experimental data of the D5-phenyl-1,1,4,4-D4-butadiene system indicate that the contribution of the atomic hydrogen loss channel from **i4** forming **p4** is only minor. This also has been confirmed via RRKM calculations (Table 2). Instead, if **i4** is formed, this intermediate rearranges solely to **i1**. Consequently, **i1** must be considered as the central reaction intermediate in the reaction of phenyl radicals with 1,3-butadiene. What is the fate of intermediate **i1**? Data from the D5-phenyl-1,3-butadiene and phenyl-D6-butadiene systems suggest the presence of two reaction channels, i.e., formation of the thermodynamically most stable 1,4-dihydronaphthalene (major product; **p3**) and of the thermodynamically less favorable product 1-phenyl-*trans*-1,3-butadiene (minor product; **p1**). Here, the aromatic 1,4-dihydronaphthalene molecule is formed from **i1** via the reaction sequence involving **i2** and **i3**. Both the experimentally determined energetics of the reaction and the tight exit transition state involved in the decomposition of **i3** to 1,4-dihydronaphthalene plus atomic hydrogen could be verified experimentally. Likewise, the “sideways scattering” as verified by a pronounced maximum of the center-of-mass angular distribution at 90° indicated geometrical constraints upon decomposition of the decomposing **i3** complex, i.e., an emission of the hydrogen atom perpendicularly to the rotation plane of the fragmenting intermediate. This has also been authenticated theoretically, and the computations depict an angle of the hydrogen atom loss of 93° with respect to the molecular plane (Figure 9). Finally, experiments and computations agree that neither the methyl nor the vinyl radical loss pathways are open.

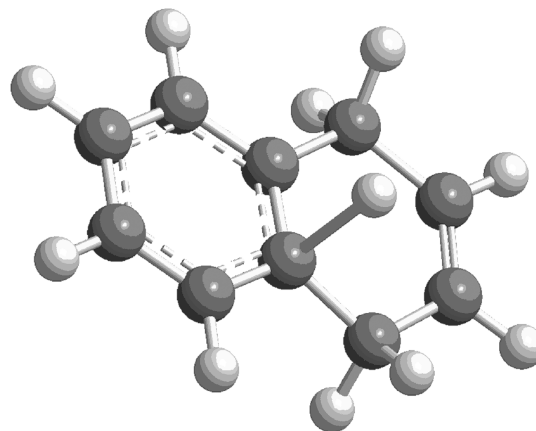


**Figure 9.** Geometry of the exit transition state forming 1,4-dihydronaphthalene.

## 5. SUMMARY

We have investigated the crossed beam reactions of the phenyl radical ( $\text{C}_6\text{H}_5$ ,  $X^2A_1$ ) with 1,3-butadiene ( $\text{C}_4\text{H}_6$ ,  $X^1A_g$ ) and D6-1,3-butadiene ( $\text{C}_4\text{D}_6$ ,  $X^1A_g$ ) as well as of the D5-phenyl radical ( $\text{C}_6\text{D}_5$ ,  $X^2A_1$ ) with 2,3-D2-1,3-butadiene and 1,1,4,4-D4-1,3-butadiene at collision energies of about 55 kJ mol<sup>-1</sup>. Experimentally and theoretically, the bicyclic and aromatic 1,4-dihydronaphthalene molecule was identified as a major product of this reaction with the 1-phenyl-1,3-butadiene being

a less prominent contributor. The reaction is initiated by a barrierless addition of the phenyl radical to the terminal carbon atom of the 1,3-butadiene (C1/C4) to form a bound intermediate; the latter underwent hydrogen elimination from the terminal CH<sub>2</sub> group of the 1,3-butadiene molecule leading to 1-phenyl-*trans*-1,3-butadiene. The dominant product, 1,4-dihydronaphthalene, is formed via an isomerization of the adduct by ring closure and emission of the hydrogen atom from the phenyl moiety at the bridging carbon atom through a tight exit transition state. The hydrogen atom was found to leave the decomposing complex almost parallel to the total angular momentum vector and perpendicularly to the rotation plane of the decomposing intermediate. The defacto barrierless formation of the 1,4-dihydronaphthalene molecule involving a single collision between a phenyl radicals and 1,3-butadiene represents an important step in the formation of PAHs and their partially hydrogenated counterparts in combustion and interstellar chemistry.

## AUTHOR INFORMATION

### Notes

The authors declare no competing financial interest.

## ACKNOWLEDGMENTS

This work was supported by the U.S. Department of Energy, Basic Energy Sciences (DE-FG02-03ER15411 to the University of Hawaii and DE-FG02-04ER15570 to Florida International University).

## REFERENCES

- (1) Richter, H.; Howard, J. B. *Prog. Energy Combust. Sci.* **2000**, *26*, 565–608.
- (2) Duley, W. W. *Faraday Discuss.* **2006**, *133*, 415–425.
- (3) Hylland, K. J. *Toxicol. Environ. Health A* **2006**, *69*, 109–123.
- (4) Frenklach, M.; Feigelson, E. D. *Astrophys. J.* **1989**, *341*, 372–384.
- (5) Tielens, A. G. G. M. *Annu. Rev. Astron. Astrophys.* **2008**, *46*, 289–337.
- (6) Hausmann, M.; Homann, K. H. *Ber. Bunsen-Ges. Phys. Chem.* **1990**, *94*, 1308–1312.
- (7) Law, M. E.; Westmoreland, P. R.; Cool, T. A.; Wang, J.; Hansen, N.; Taatjes, C. A.; Kasper, T. *Proc. Combust. Inst.* **2007**, *31*, 565–573.
- (8) Yu, T.; Lin, M. C. J. *Phys. Chem.* **1995**, *99*, 8599–8603.
- (9) Yu, T.; Lin, M. C. *Combust. Flame* **1995**, *100*, 169–176.
- (10) Park, J.; Nam, G. J.; Tokmakov, I. V.; Lin, M. C. *J. Phys. Chem. A* **2006**, *110*, 8729–8735.
- (11) Tokmakov, I. V.; Park, J.; Lin, M. C. *ChemPhysChem* **2005**, *6*, 2075–2085.
- (12) Park, J.; Wang, L.; Lin, M. C. *Int. J. Chem. Kinet.* **2003**, *36*, 49–56.
- (13) Park, J.; Burova, S.; Rodgers, A. S.; Lin, M. C. *Chem. Phys. Proc. Combust.* **1999**, 308–311.
- (14) Ismail, H.; Park, J.; Wong, B. M.; Green, W. H., Jr.; Lin, M. C. *Proc. Combust. Inst.* **2005**, *30*, 1049–1056.
- (15) Frenklach, M. *Phys. Chem. Chem. Phys.* **2002**, *4*, 2028–2037.
- (16) Miller, J. A.; Melius, C. F. *Combust. Flame* **1992**, *91*, 21–39.
- (17) Kaiser, R. I. *Chem. Rev.* **2002**, *102*, 1309–1358.
- (18) Park, J.; Tokmakov, I. V.; Lin, M. C. *J. Phys. Chem. A* **2007**, *111*, 6881–6889.
- (19) Zhang, F.; Gu, X.; Guo, Y.; Kaiser, R. I. *J. Phys. Chem. A* **2008**, *112*, 3284–3290.
- (20) Gu, X.; Zhang, F.; Guo, Y.; Kaiser, R. I. *J. Phys. Chem. A* **2007**, *111*, 11450–11459.
- (21) Zhang, F.; Gu, X.; Guo, Y.; Kaiser, R. I. *J. Org. Chem.* **2007**, *72*, 7597–7604.
- (22) Gu, X.; Kaiser, R. I. *Acc. Chem. Res.* **2009**, *42*, 290–302.
- (23) Gu, X.; Zhang, F.; Kaiser, R. I. *J. Phys. Chem. A* **2009**, *113*, 998–1006.
- (24) Kohn, D. W.; Clauberg, H.; Chen, P. *Rev. Sci. Instrum.* **1992**, *63*, 4003–4005.
- (25) Stranges, D.; Stemmler, M.; Yang, X.; Chesko, J. D.; Suits, A. G.; Lee, Y. T. *J. Chem. Phys.* **1998**, *109*, 5372–5382.
- (26) Li, Y.; Zhang, L.; Tian, Z.; Yuan, T.; Wang, J.; Yang, B.; Qi, F. *Energy Fuels* **2009**, *23*, 1473–1485.
- (27) Mebel, A. M.; Kislov, V. V. *J. Phys. Chem. A* **2009**, *113*, 9825–9833.
- (28) Kislov, V. V.; Mebel, A. M. *J. Phys. Chem. A* **2010**, *114*, 7682–7692.
- (29) Parker, D. S. N.; Zhang, F.; Kim, Y. S.; Kaiser Ralf, I.; Landera, A.; Kislov, V. V.; Mebel, A. M.; Tielens, A. G. G. M. *Proc. Natl. Acad. Sci. U.S.A.* **2011**, *109*, 53–58.
- (30) Parker, D. S. N.; Zhang, F.; Kaiser, R. I.; Kislov, V. V.; Mebel, A. M. *Chem.—Asian J.* **2011**, *6*, 3035–3047.
- (31) Kaiser, R. I.; Parker, D. S. N.; Goswami, M.; Zhang, F.; Kislov, V. V.; Mebel, A. M.; Aguilera-Iparraguirre, J.; Green, W. H. *Phys. Chem. Chem. Phys.* **2011**, *14*, 720–729.
- (32) Gu, X.; Guo, Y.; Kawamura, E.; Kaiser, R. I. *J. Vac. Sci. Technol., A* **2006**, *24*, 505–511.
- (33) Gu, X.; Guo, Y.; Zhang, F.; Mebel, A. M.; Kaiser, R. I. *Faraday Discuss.* **2006**, *133*, 245–275.
- (34) Guo, Y.; Gu, X.; Kawamura, E.; Kaiser, R. I. *Rev. Sci. Instrum.* **2006**, *77*, 034701/034701–034701/034709.
- (35) Kaiser, R. I.; Matsyutenko, P.; Ennis, C.; Zhang, F.; Gu, X.; Mebel, A.; Kostko, O.; Ahmed, M. *Faraday Discuss.* **2010**, *147*, 429–478.
- (36) Zhang, F.; Kim, S.; Kaiser, R. I. *Phys. Chem. Chem. Phys.* **2009**, *11*, 4707–4714.
- (37) Vernon, M. Ph. D. Thesis, University of California, Berkeley, 1981.
- (38) Weiss, M. S. Ph. D. Thesis, University of California, Berkeley, 1986.
- (39) Becke, A. D. *J. Chem. Phys.* **1993**, *98*, 5648–5652.
- (40) Lee, C.; Yang, W.; Parr, R. G. *Phys. Rev. B* **1988**, *37*, 785–789.
- (41) Baboul, A. G.; Curtiss, L. A.; Redfern, P. C.; Raghavachari, K. J. *Chem. Phys.* **1999**, *110*, 7650–7657.
- (42) Curtiss, L. A.; Raghavachari, K.; Redfern, P. C.; Baboul, A. G.; Pople, J. A. *Chem. Phys. Lett.* **1999**, *314*, 101–107.
- (43) Curtiss, L. A.; Raghavachari, K.; Redfern, P. C.; Rassolov, V.; Pople, J. A. *J. Chem. Phys.* **1998**, *109*, 7764–7776.
- (44) Frisch, M. J.; Trucks, G. W.; Schlegel, H. B.; Scuseria, G. E.; Robb, M. A.; Cheeseman, J. R.; Zakrzewski, V. G.; Montgomery, J. A.; Stratmann, Jr., R. E.; Burant, J. C. et al. *Gaussian 98*, revision A.11; Gaussian, Inc.: Pittsburgh, PA, 1998.
- (45) Werner, H.-J.; Amos, R. D.; Bernhardsson, A.; Berning, A.; Celani, P.; Cooper, D. L.; Deegan, M. J. O.; Dobbyn, A. J.; Eckert, F.; Hampel, C. et al. *MOLPRO, A Package of Ab Initio Programs*, version 2006.1; MOLPRO: Cardiff, U.K., 2006 ([www.molpro.net](http://www.molpro.net)).
- (46) Jensen, H. J. Aa.; Ågren, H.; Olsen, J. SIRIUS: a general-purpose direct second-order MCSCF program. In *Modern Techniques in Computational Chemistry*; Clementi, E., Ed.; ESCOM: Leiden, The Netherlands, 1991.
- (47) Angeli, C. et al. *Dalton, A Molecular Electronic Structure Program*, release 2.0, 2005; see <http://www.kjemi.uio.no/software/dalton/dalton.html>.
- (48) Werner, H.-J. *Mol. Phys.* **1996**, *89*, 645–661.
- (49) Eyring, H.; Lin, S. H.; Lin, S. M. *Basic Chemical Kinetics*; John Wiley and Sons, Inc.: New York, 1980.
- (50) Robinson, P. J.; Holbrook, K. A. *Unimolecular Reactions*; John Wiley and Sons, Ltd.: New York, 1972.
- (51) Steinfeld, J.; Francisco, J.; Hase, W. *Chemical Kinetics and Dynamics*; Prentice Hall: Englewood Cliffs, NJ, 1982.
- (52) Kislov, V. V.; Nguyen, T. L.; Mebel, A. M.; Lin, S. H.; Smith, S. C. *J. Chem. Phys.* **2004**, *120*, 7008–7017.
- (53) Levine, R. D. *Molecular Reaction Dynamics*; Cambridge University Press: Cambridge, UK, 2005.

(54) Miller, W. B.; Safron, S. A.; Herschbach, D. R. *Discuss. Faraday Soc.* **1967**, *44*, 108–122.

(55) Fascella, S.; Cavallotti, C.; Rota, R.; Carra, S. *J. Phys. Chem. A* **2004**, *108*, 3829–3843.

(56) Linstrom, P. J.; Mallard, W. G., Eds. *NIST Chemistry WebBook*; NIST Standard Reference Database Number 69; NIST: Gaithersburg, MD, 2005. (<http://webbook.nist.gov/chemistry/>).

(57) Pedley, J. B.; Naylor, R. D.; Kirby, S. P. *Thermochemical Data of Organic Compounds*, 2nd ed.; Chapman and Hall: London, 1986.

(58) Taskinen, E. *J. Phys. Org. Chem.* **2008**, *22*, 632–642.